Observing the Period and Period Derivative of the Crab Pulsar (B0531+21)

James Michael Patrick Brady
ID: 10459769
School of Physics and Astronomy
The University of Manchester
Experiment conducted with Joshua Whittaker, ID: 10634777
(Dated: December 2022)

The Crab Pulsar, B0531+21, was observed multiple times over a period of two weeks, to observe its period derivative and hence infer its surface magnetic field strength and characteristic age. Dispersion of the signals indicated that the distance to the pulsar was on the order 1900 ± 20 kpc, which is close to the accepted value of 2 kpc. The signal was then corrected to the barycentre of the solar system and the remainders of the delayed times were tracked to find accurate periods. It was found that the Crab Pulsar's period increases at a rate of 0.4337 ± 0.1282 ps/s , producing a surface magnetic field strength of 389.8 ± 3.42 MT and a characteristic age of 1230 ± 21.8 yr , all of which are within acceptable ranges.

I. INTRODUCTION

Pulsars are highly useful objects to observe in radio astronomy. First discovered by Bell and Hewish in 1968 [1], they are stellar remnants with a strong and rapidly spinning magnetic field, which produces two beams of charged particles with a highly regular period. As a result, pulsars are very convenient references for timing astrophysical events and measuring distances at both a galactic and intergalactic scale (via dispersion and Doppler shifting respectively). Pulsars are also being used to observe behaviours at the fringes of known physics, such as gravitational waves and black hole interactions. Through the experiment, we aimed to find the distance to the Crab Pulsar from the dispersion of its signal, use the solar barycentre as a reference to directly find its period and period derivative and hence infer its surface magnetic field strength and characteristic age.

II. DE-DISPERSION OF SIGNALS

The ISM situated throughout the galaxy is slightly ionised, which leads to the dispersion of electromagnetic radiation of frequency ν (Hz) and pulse period P (s) travelling through it. The dispersion relation is given as:

$$t_{delay} = \frac{P}{\Phi} = \frac{DM}{2.410 \times 10^{-4} \nu_{MHz}^2} \tag{1}$$

where DM is the dispersion measure (cm^{-3}pc) and Φ is the phase along the period (between 0 and 1) [2]. The dispersion measure is defined for an electron number density n_e (cm^{-3}) and distance R (pc) as:

$$DM = \int_0^R n \, dl \tag{2}$$

For dispersed data, the dispersion measure can be found from the gradient of the linear fit of t_{delay} against $\nu^{-2}$and hence the distance to the pulsars can also be found [3]. The data was collected and binned into 1024 discrete bins of phase by the 12.8m diameter radio telescope, operating at a central frequency ν_0 of 610 MHz and bandwidth B of 10 MHz. A number density of 0.03cm^{-3} is assumed. The error on the dispersion measure was found by propagating the uncertainties on the pulse length (defined to 500μs) and phase (defined to half a bin width) and fitted values were compared to those of the CSIRO Pulsar Database [4]. The reference distance of the Crab Pulsar as according to the CSIRO database is 2kpc, the values as seen in Table I are near to this reference value but are not included within error. In addition, the values of χ^2_{red} are outside of the ideal range, indicating that there is a source of error not accounted for by estimating the accuracy from the data. Once the data has been dedispersed, the methods outlined by Taylor can be used to

DM (pc cm^{-3})	χ^2_{red}	Distance (pc)
56.5 ± 1.18	4.6	1880 ± 40
57.8 ± 0.66	4.1	1930 ± 22
56.3 ± 3.32	3.6	1880 ± 110

TABLE I: The dispersion measures found for each observation of the Crab Pulsar, alongside their relevant χ^2_{red} from fitting and respective distances.

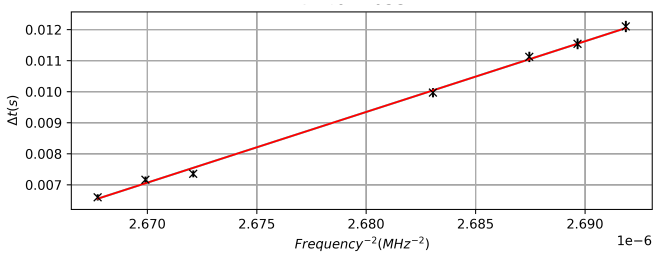

FIG. 1: A linear fit for the dispersion measure of the Crab Pulsar performed using LSFR.py

calculate the times of arrivals of each sub-integration of the data as well as the approximate errors on those times [5].

III. CORRECTING TO THE SOLAR BARYCENTRE

Although dispersion has been accounted for, the time delay due to physical distance between the observatory and the solar barycentre has not been corrected for. The barycentre of the solar system provides a convenient reference point for observation, as it is approximately static with respect to the Crab Pulsar if received radiation can be approximated as a plane wave. However, the signal was observed at Jodrell Bank, rather than the barycentre and so experiences a time delay that can be split into two parts - the Roemer Delay, which is between the solar barycentre and the centre of the Earth and a positional delay due to the distance between the centre of the earth and the observatory [6]. The delay due to the position of the observatory for an observed elevation of the Crab Pulsar ϵ as shown in Figure 2 is given by:

$$\Delta t_{obs} = \frac{R_E \sin \epsilon}{c} \tag{3}$$

where ϵ varies with the times of arrival of the pulses, found by using AstroPy's coordinate transformation methods and a the reference position of the Crab Pulsar [7]. Similarly, the Roemer Delay is shown in Figure 3 and is given by:

$$\Delta t_{Roemer} = \frac{\hat{p} \cdot \underline{r}}{c} \tag{4}$$

where $\hat{p}$ is the unit vector pointing to the Crab Pulsar from the barycentre and $\underline{r}$ is the vector pointing to the centre of the Earth from the barycentre (with units AU). Whilst the components of $\underline{r}$ are found from the Astronomical Almanac, the positions need to be interpolated for each time of arrival for the most accurate results [8]. The Lagrange Three Point Formula was used to interpolate over a time period of two days, being the simplest and most general form that produced an error of 0.05ms from the remainder to a boundary observation error of 0.2ms from the corresponding remainder. Hence, the delays can be found for all times of arrivals and so they can be corrected to allow for the analysis of the period derivative. Whilst increasing the degree of interpolation would reduce the remainder, it would be unnecessary, as the remainder is already suitably below the boundary and those generated through calculating the times of arrivals are comparable (on the order of 10 - 100 μs). Overall, the Roemer Delay is the more significant of the two delays.

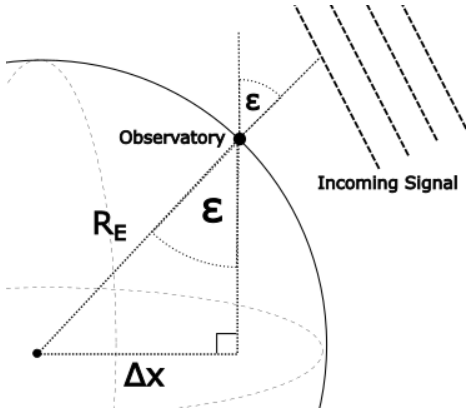

FIG. 2: A diagram demonstrating the delay due to the position of the observatory relative to the centre of the Earth. This diagram was created by the author of this document.

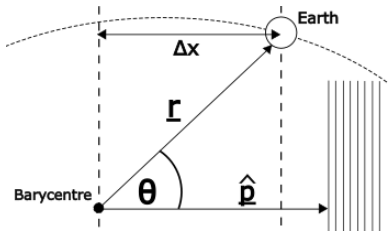

FIG. 3: A diagram demonstrating Roemer Delay. This diagram was created by the author of this document.

IV. OBSERVING THE CRAB PULSAR

Once the data has been dedispersed and corrected to the solar barycentre, the period and period derivative of the pulsar can be observed. For a packet of pulses observed over a time t from a reference time t_0, an integer number of pulses should be observed:

$$N = \frac{t - t_0}{P} \tag{5}$$

The errors on these period residuals are propagated directly from the errors on the time of arrivals and the remainder of the interpolation. However, if an non-integer number of pulses is observed, it is likely that the period

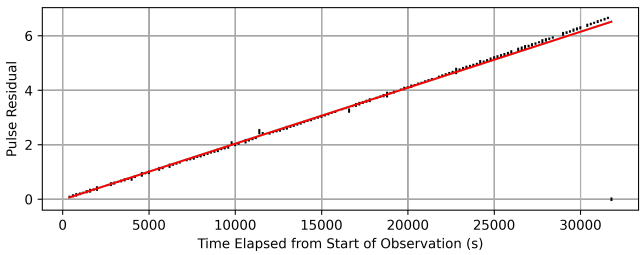

FIG. 4: Uncorrected residuals for the data recorded on 23/11, with a straight line fitted across the data points

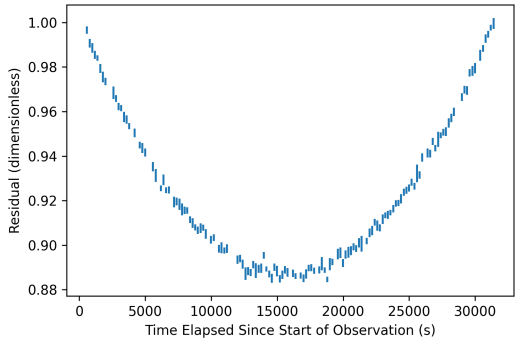

FIG. 5: Residuals for the data in 4 after the period has been corrected.

TABLE II: The true periods of the Crab Pulsar as calculated on each of the dates listed

Dates (dd/mm, 2022)	True Period (ms)	Period Error (ns)
16/11	33.808469	23.11
23/11	33.808737	1.40
27/11	33.808881	5.99

of the pulsar is different to the expectation. If there is some change in the period, ΔP, it should be related to the gradient of the linear fit of $t - t_0$ against the period residuals:

$$\Delta P = P^2 \frac{\Delta N}{\Delta t} \tag{6}$$

. From Figure 5, once the linear fit has been performed, a clear quadratic relation is seen in the residuals, because the quadratic term of a Taylor Expansion is the next most simple term remaining once the linear term has been eliminated. Data sets separated over days of observation allow for an approximate value for the period derivative to be found:

$$\frac{dP}{dt} = \dot{P} \approx \frac{\Delta P_{true}}{\Delta t} \tag{7}$$

From Table II, the average value of $\dot{P}$ is found to be 0.4337 ± 0.1282 ps/s, indicating that the rotation of the Crab Pulsar is slowing down. The observed period derivative is within tolerance of the value provided by the CSIRO Pulsar Database, citing a value of $\dot{P}$ of 0.421 ps/s [4]. The rotation is likely to be slowing down due to radiation through the sweeping beam removing energy and gravitational waves. The period derivative can be used to calculate the approximate surface magnetic field strength, B_0 of the Crab Pulsar (in T):

$$B_0 \approx 3.2 \times 10^8 \left(\frac{R}{10\text{km}}\right)^{-3} \left(\frac{I}{10^{38}\text{kgm}^2}\right)^{\frac{1}{2}} \sqrt{P\dot{P}} \tag{8}$$

and the characteristic age of the Crab Pulsar (in s):

$$\tau_{ch} \approx \frac{P}{2\dot{P}} \tag{9}$$

Using the true period of the Crab Pulsar as of 27/11, the surface magnetic field strength is calculated to be 389.8 ± 3.42 MT and the characteristic age as 1230 ± 21.8 yr. The CSIRO Pulsar Catalogue notes that the surface field strength of the Crab Pulsar is 379 MT and that its characteristic age is 1260 yr, hence the observations made over the course of the experiment are suitably precise and accurate [4].

V. CONCLUSION

The Crab Pulsar has been successfully observed over several days using the 12.8m telescope at Jodrell Bank. Dedispersion through linear fitting allowed for distances of the order 1.9 ± 0.02 kpc to be found. These are close to the reference distance of 2 kpc, but slightly outside tolerance, indicating a minor source of error, which might be rectified by using a variable ISM electron density. Assuming minimal parallax and using the Lagrange Three Point Formula, the delay times to the solar barycentre could be found using this dedispersed data. After correcting for the delays and correcting the period through lineraly fitting the residuals, a period derivative of 0.4337 ± 0.1282 ps/s was found. Using approximate relations, a surface magnetic field strength of 389.8 ± 3.42 MT and a characteristic age of 1230 ± 21.8 yr, which are both within acceptable ranges.

[1] A. Hewish, S. Bell, *et al.*, Observation of a rapidly pulsating radio source, Nature **217**, 709 (1968).

[2] A. Lyne, F. Graham-Smith, and B. Stappers, Pulsar astronomy (Cambridge University Press, Cambridge, 2022) Chap. 3, 5th ed.

[3] A. Lyne, F. Graham-Smith, and B. Stappers, Pulsar astronomy (Cambridge University Press, Cambridge, 2022) Chap. 7, 5th ed.

[4] R. Manchester, G. B. Hobbs, A. Teoh, *et al.*, The australia telescope national facility pulsar catalogue, The Astronomical Journal **129**, 1993 (2005).

[5] J. Taylor, Pulsar timing and relativistic gravity, Philosophical Transactions: Physical Sciences and Engineering **341** (1992).

[6] A. Lyne, F. Graham-Smith, and B. Stappers, Pulsar astronomy (Cambridge University Press, Cambridge, 2022) Chap. 5, 5th ed.

[7] F. Ochsenbein, P. Bauer, and J. Marcout, The vizier database of astronomical catalogues, Astronomy and Astrophysics Supplement Series **143**, 23 (2000).

[8] H. M. N. A. Office, *Astronomical Almanac 2022, The* (UK Hydrographic Office, 2022).